ACS APPLIED MATERIALS & INTERFACES

Research Article

www.acsami.org

Mussel-Inspired One-Step Adherent Coating Rich in Amine Groups for Covalent Immobilization of Heparin: Hemocompatibility, Growth Behaviors of Vascular Cells, and Tissue Response

Ying Yang,[†,‡] Pengkai Qi,[†,‡] Feng Wen,[§] Xiangyang Li,[†,‡] Qin Xia,[†,‡] Manfred F. Maitz,[†,⊥] Zhilu Yang,*[,†,‡] Ru Shen,[†,‡] Qiufen Tu,[†,#] and Nan Huang*[,†,‡]

[†]Key Laboratory of Advanced Technology for Materials of Education Ministry, [‡]The Institute of Biomaterials and Surface Engineering, School of Materials Science and Engineering, and [#]Laboratory of Biosensing and MicroMechatronics, Southwest Jiaotong University, Chengdu 610031, China

[§]Key Laboratory of Advanced Materials of Tropical Island Resources of Ministry of Education, School of Materials and Chemical Engineering, Hainan University, Haikou 570228, China

[⊥]Max Bergmann Center of Biomaterials, Leibniz Institute of Polymer Research Dresden, Hohe Strasse 6, 01069 Dresden, Germany

Supporting Information

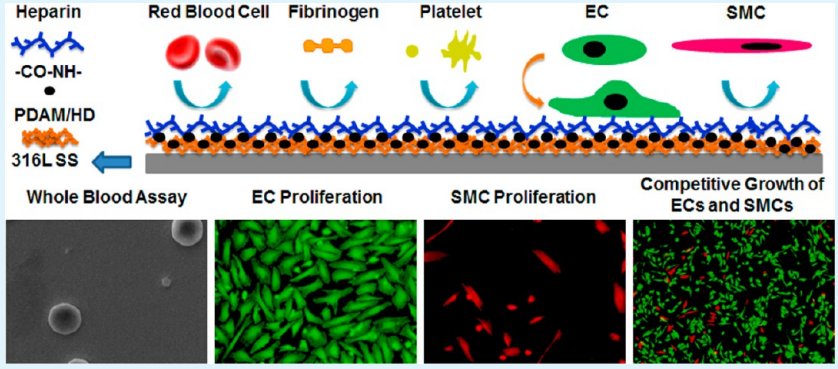

ABSTRACT: Heparin, an important polysaccharide, has been widely used for coatings of cardiovascular devices because of its multiple biological functions including anticoagulation and inhibition of intimal hyperplasia. In this study, surface heparinization of a commonly used 316L stainless steel (SS) was explored for preparation of a multifunctional vascular stent. Dip-coating of the stents in an aqueous solution of dopamine and hexamethylendiamine (HD) (PDAM/HD) was presented as a facile method to form an adhesive coating rich in primary amine groups, which was used for covalent heparin immobilization via active ester chemistry. A heparin grafting density of about 900 ng/cm^2 was achieved with this method. The retained bioactivity of the immobilized heparin was confirmed by a remarkable prolongation of the activated partial thromboplastin time (APTT) for about 15 s, suppression of platelet adhesion, and prevention of the denaturation of adsorbed fibrinogen. The Hep-PDAM/HD also presented a favorable microenvironment for selectively enhancing endothelial cell (EC) adhesion, proliferation, migration and release of nitric oxide (NO), and at the same time inhibiting smooth muscle cell (SMC) adhesion and proliferation. Upon subcutaneous implantation, the Hep-PDAM/HD exhibited mitigated tissue response, with thinner fibrous capsule and less granulation formation compared to the control 316L SS. This number of unique functions qualifies the heparinized coating as an attractive alternative for the design of a new generation of stents.

KEYWORDS: *heparin, primary amine-rich coating, hemocompatibility, endothelial cell selectivity, competitive adhesion, multifunctional stent*

1. INTRODUCTION

Cardiovascular diseases (CVDs), mainly caused by atherosclerosis, present a major cause of death worldwide. Atherosclerosis (AS) is a chronic inflammatory disease of the artery wall, where both the innate and adaptive immune responses contribute to the disease initiation and progression. Interventional treatments of CVDs with vascular stents emerged as minimal invasive alternatives to the traditional bypass surgery. However, besides all the immediate benefits, the stent implantation also provokes injury-induced inflammation, proliferation and migration of smooth muscle cells (SMCs), neointimal hyperplasia and subsequent in-stent restenosis (ISR).[1] The application of drug-eluting stents (DES) has been reported to effectively decrease the incidence of ISR by

Received: June 19, 2014
Accepted: August 8, 2014
Published: August 8, 2014

50−70%.[2,3] Nevertheless, the drugs loaded on DES delayed vascular healing and re-endothelialization, which resulted in high risk of late thrombosis.[4]

Endothelial cells (ECs) play key roles in maintaining vascular homeostasis. First, the primary physiological function of ECs is to provide an appropriate hemo-compatible surface to guarantee blood flow.[5] Additionally, healthy endothelium effectively controls SMCs proliferation.[6,7] Thus, a balanced behavior of ECs and SMCs for reduced thrombosis and restenosis of a stent can be obtained by selective promotion of ECs in competitive adhesion with SMCs.[8,9]

Heparin, an important polysaccharide,, is a structural mimic of the proteoglycan heparan sulfate, which is a major anticoagulant on the endothelial surface in all tissues.[10] Heparin has been employed clinically as an anticoagulant since 1935, and the anticoagulant mechanism of heparin depends on the potential to preferentially interact with antithrombin III (ATIII) and the ability of this heparin-ATIII complex to inhibit key components in the coagulation cascade such as Factor Xa and thrombin (Factor IIa).[11,12] Additionally, heparin has been reported to be an anti-inflammatory drug in various models of inflammatory diseases in the 1960s.[13,14] Today, heparin has a broad spectrum of applications, from the original use as soluble anticoagulant, via a surface-grafted anticoagulant to structure forming components in electrostatic layer-by-layer assemblies or in hydrogels.[15,16] These applications also take use of the affinity of fibronectin and growth factors like vascular endothelial growth factor (VEGF) and epidermal growth factor (EGF) to heparin and set up drug delivery systems or stimulate cell differentiation.[17−20] Various technologies have been developed to provide heparin as stable coatings, or in nonregulated or feedback-controlled coagulation regulated release systems.[17,21]

Heparin also has the ability to suppress SMCs adhesion and proliferation. Several *in vitro* studies reported that heparin prevents intimal hyperplasia.[22,23] However, there were conflicting reports about the influence of heparin on the growth of ECs. Heparin was partly considered to harm EC growth according to certain studies.[24,25] However, Azizkhan et al.[26] have reported that heparin possessed the ability to promote bovine capillary endothelial cell migration but had no impact on the proliferation. Our recent studies reported that a surface tailored with heparin in a proper concentration could not only improve hemocompatibility and inhibit SMC proliferation but also enhance EC growth.[15,27] However, there have been no reports about how a heparinized surface influences the competitive adhesion of ECs and SMCs.

The aim of this work was to develop a heparinized surface and investigate the effect on hemocompatibility, growth of vascular cells, and tissue response. However, stent materials usually lack functional groups for anchoring biomolecules. Polydopamine (PDAM) is a functional coating inspired by the secreted adhesive proteins of mussels with high 3,4-dihydroxy-L-phenylalanine (DOPA) and lysine content, which has attracted great attention in the biomaterials field, because of its ability to bind strongly to almost all kinds of substrates and provide secondary reactivity for anchoring amine- or sulfhydryl group containing biomolecules.[28−30] The PDAM-based platform could also be used to graft heparin by dopamine-conjugated heparin (hepamine) technology.[31,32] However, the PDAM coating does not provide sufficient amine groups to directly conjugate heparin.[17,31,32] For extended possibilities to immobilize also biomolecules containing carboxyl groups, we developed a functional polymer coating in a one-step process by copolymerization of dopamine and hexamethylendiamine (HD) (PDAM/HD), which presents abundant amine groups for chemical conjugation.[33] Heparin then was covalently immobilized on the PDAM/HD coating through the reaction of the primary amine groups of the PDAM/HD with the carbodiimide activated carboxylic groups of heparin. This provides a surface with multiple biofunctionalities, which can be applied as stent coating. In this study, the hemocompatibility, growth behaviors, competitive adhesion of vascular cells, and host tissue response to the heparin-functionalized PDAM/HD coating were systematically investigated.

2. EXPERIMENTAL SECTION

Preparation of PDAM/HD Coating. The copolymer coating of PDAM/HD was deposited on mirror polished 316L SS (Φ10 mm) through dip-coating as described before.[28] In brief, dopamine hydrochloride (1 mg/mL) and HD (2.44 mg/mL) were successively dissolved in Tris buffer (1.2 mg/mL, pH 8.5). Then the 316L SS substrates were immersed into the above mixed solution. After deposition for 48 h at 20 °C, the specimens were washed in distilled water (6 times, 5 min) to remove loosely adsorbed polymers. For the deposition of the control PDAM, 1 mg/mL of dopamine hydrochloride was used and dissolved in Tris buffer (pH 8.5), and the remaining process was equal as above. The as-deposited PDAM and PDAM/HD coatings were subsequently thermally treated at 120 °C under 5×10^{-4} Pa for 1 h.

Characterization of the Coating. The surface chemical compositions of the specimens were measured by X-ray photoelectron spectroscopy (XPS, K-Alpha, Thermo Electron, USA). The instrument was equipped with a monochromatic Al Kα (1486.6 eV) X-ray source operated at 12 kV × 15 mA at a pressure of 3×10^{-7} Pa. The graphitic carbon peak (285 eV) was used as a reference for charge correction.

Colorimetric staining with Acid Orange II (AO II) was used to determine amine groups.[32] The thickness of the coating was detected by a spectroscopic ellipsometer (M-2000 V, J.A. Woollam, USA) using Cauchy model. Δ and Ψ values were measured at a wavelength of 370−1000 nm.

Heparin Conjugation and Quantification. One mg/mL of heparin sodium salt (Potency ≥150 IU/mg, Sigma-Aldrich) was in advance activated in water-soluble carbodiimide (WSC) solution composed of 1 mg/mL *N*-(3-dimethylaminopropyl) -*N*′-ethylcarbodiimide (EDC, purity ≥98.0%, Sigma-Aldrich), 0.24 mg/mL *N*-hydroxysuccinimide (NHS, purity ≥97.0%, Sigma−Aldrich), and 9.76 mg/mL 2-(*N*-morpholino)ethanesulfonic acid hydrate (MES, Purity ≥97.0%, Sigma−Aldrich) for 15 min. Then, the 316L SS coated with PDAM/HD were immersed into the above heparin sodium salt solution for incubation. After reaction for 12 h, the specimens were washed with phosphate buffered saline (PBS) (3 times, 5 min) and distilled water (3 times, 5 min) before surface analysis.

The amount of heparin bound to the surface of coating was determined by a Toluidine blue-O (TBO) method.[16] The stability of the heparin bound to the PDAM/HD coating was evaluated by XPS quantification of the surface sulfur content of Hep-PDAM/HD before and after immersion in PBS at 37 °C under constant agitation.

Hemocompatibility. Fresh human venous blood used in hemocompatibility evaluation was obtained from Blood Center of Chengdu, PR China in agreement with ethic rules. The blood was anticoagulated with trisodium citrate in a 9:1 volumetric ratio and all experiments were carried out within 12 h after the blood donation. All of the tests were performed at least twice with more than four parallel samples.

Platelet poor plasma (PPP) was obtained by centrifugation (3000 rpm, 15 min) of fresh human whole blood. Fibrinogen (Fg) adsorption was evaluated by incubating the samples with PPP (50 μL) at 37 °C for 120 min.[34] The exposure of γ chain of adsorbed Fg was determined by indirect immunochemistry using the conformation

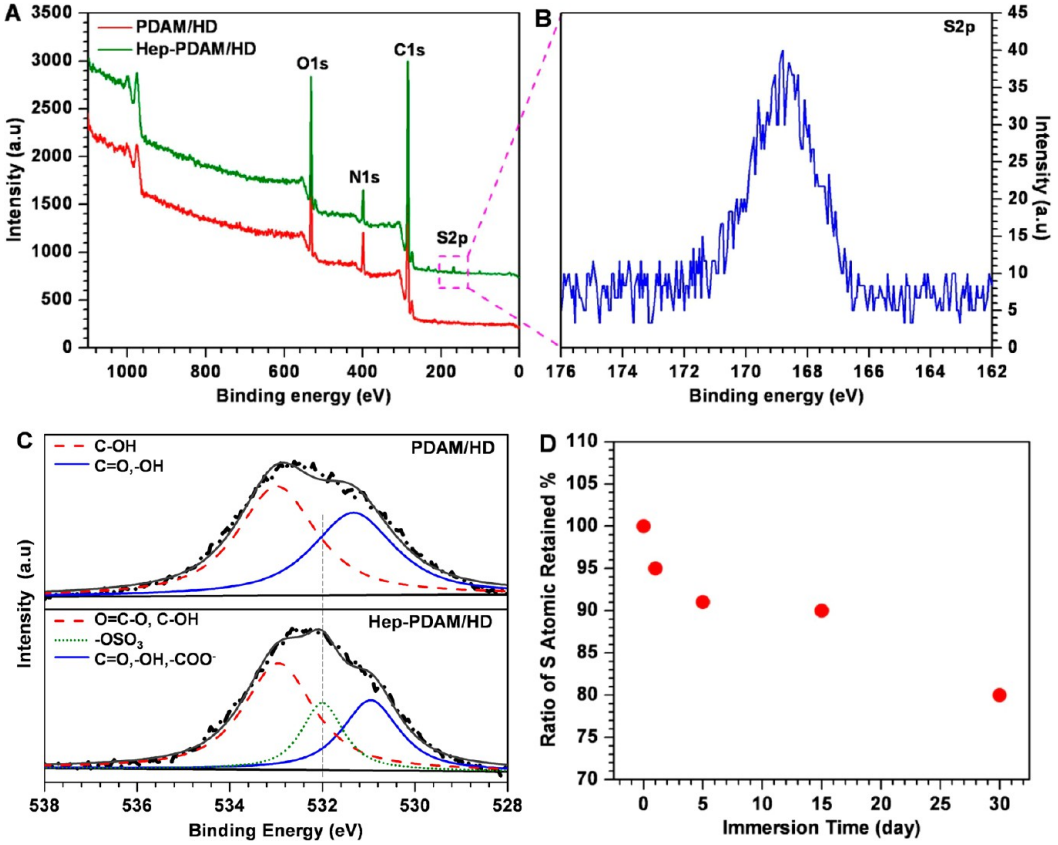

Figure 1. (A) XPS wide scans and (B) S 2p high-resolution spectra of the PDAM/HD coating before and after heparin conjugation; (C) comparison of the O 1s high-resolution spectra of the PDAM/HD coating before and after heparin conjugation; (D) relative amounts of heparin retained on Hep-PDAM/HD surfaces after immersion in PBS for various periods of time (represented by S atomic %, with 0 day set as 100%).

sensitive primary antibody NYB4-2xl-f (ACCURATE Chemical) as described before.[34]

For determination of the activated partial thromboplastin time (APTT), the samples were incubated with 350 μL PPP for 30 min at 37 °C. Then, the clotting time of the plasma was measured by a coagulometer (ACL 200, Instrumentation Laboratory Co. USA) with APTT kit.

Platelet-rich plasma (PRP) was obtained by slow centrifugation (1500 rpm, 15 min) of fresh human whole blood. Fifty microliters of fresh PRP was added on the samples (10 mm diameter) and incubated for 2 h at 37 °C in humidified air. After rinsing with 0.9% NaCl solution, they were fixed in 2.5% glutaraldehyde solution overnight, then dehydrated and dealcoholized. After critical point drying, samples were processed for field-emission scanning electron microscopy (SEM, JSM-7001F, JEOL Ltd., Japan).

Expression of the platelet activation marker platelet P-selectin on material surfaces, was determined by indirect immunofluorescence as described elsewhere.[34] The amount of platelets adherent on the sample surfaces was determined by measuring the lactate dehydrogenase (LDH) activity, released from the adherent cells upon lysis with Triton X-100.[34] Whole blood experiment was carried out under flow conditions using a modified Chandler-Loop.[34]

HUVEC Culture. Harvested primary HUVECs from human umbilical veins were cultured in a humidified incubator under 5% CO_2 at 37 °C using DMEM-F12 medium supplemented with 15% FBS and 20 μg/mL endothelial cell growth supplement (ECGS, Millipore, Inc.).

HUVECs were seeded on the surfaces of the samples at a density of 5×10^4 cells/cm^2 (measured using a hemocytometer). Samples were removed for analysis after 2 h, 1 and 3 days of incubation, washed, and fixed with 2.5% glutaraldehyde overnight. For cell fluorescence staining, all the samples were washed with PBS, incubated with Rhodamine123 for 15 min (20 μg/mL in PBS, Sigma-Aldrich). After three times washing with PBS, the cells were inspected and photographed using a Leica DMRX fluorescence microscope (DMRX, Leica, Germany). The number of HUVECs attached onto the sample was determined from at least 12 images. Minor/major axis ratio and projected area per cell were calculated from at least 120 cells from six random fields. HUVEC proliferation was investigated by Cell Counting Kit-8 (CCK-8) after incubation for 1 and 3 days, respectively.[27]

For NO detection, HUVECs were seeded at high density (5×10^5 cells/cm^2) onto each sample to ensure the formation of a confluent monolayer, after adhesion for 6 h, all the samples were transferred to new culture plates and 1 mL of fresh culture medium was added. After 6, 18, and 42 h, 150 μL of culture medium was collected. All the collected culture media were stored at −20 °C until analysis. NO release was determined using Griess reagent (Sigma).[34]

A HUVEC migration assay was performed as described in elsewhere,[34] HUVECs were seeded at a density of 5×10^5 cells/cm^2 on one arm of L-shaped sample disks. After 6 h, the samples were turned and cells could migrate to the other arm. After 1 day, the cells were fixed and Rhodamine123 stained, thus evaluated by a fluorescence microscope.

HUASMC Culture. Primary cultures of human umbilical artery smooth muscle cells (HUASMCs) were obtained by slow outgrowth from small pieces of umbilical artery media under standard cell culture conditions in DMEM/F12 medium with 10% FBS. The culture medium was changed every 3 days. Subculture was performed when a degree of confluency >80% was obtained, and cells between second and fifth passage were used.

HUASMCs were seeded on samples at a density of 5×10^4 cells/cm^2. The samples were respectively taken out after 2 h, 1 and 3 days of incubation, washed, and fixed with 2.5% glutaraldehyde overnight. Cell staining was performed according to the procedure as described above. HUASMC proliferation was investigated by Cell Counting Kit-8

(CCK-8) after incubation for 1 and 3 days, respectively, as described above.

The HUASMCs migration assay was performed as HUVECs migration assay described above.

Competitive Adhesion of HUVECs and HASMCs. Cell trackers with different colors were used to distinguish HUVECs (Green chloromethylfluorescein diacetate, CMFDA) and HASMCs (Orange chloromethyl trimethyl rhodamine, CMTMR) in the coculture assay.[35] Cells were incubated with the cell tracker dyes for labeling and then seed on the samples by mixing the HUVECs and HASMCs suspensions at a volume rate of 1:1 using DMEM-F12 medium supplemented with 10% FBS. The densities of both kinds of cells were 5×10^4 cells/cm^2 each.[36] The competitive cell adhesion was examined after 2 h incubation in a humidified atmosphere with 5% CO_2 and 95% air. The cells were inspected and photographed using fluorescence microscope. The average density of adherent cells was determined from more than 12 images.

***In Vivo* Subcutaneous Implantation Studies.** All animal experiments were carried out in accordance with protocols approved by the Local Ethical Committee and Laboratory Animal Administration Rules of China. Four healthy New Zealand white rabbits (weight about 4 kg, aged from 9 to 10 months) were used. Bare 316L SS disks (3×4 mm^2, both surfaces mirror-polished) and 316L SS disks with PDAM/HD coating, Hep-PDAM/HD coating were subcutaneously implanted on both sides of the back. After 2 and 9 weeks, the samples with the surrounding tissues were excised to evaluate the tissue responses in situ. The collected tissues were fixed in 10% formaldehyde for 2−3 days. The metal samples were removed and the remaining tissues were thoroughly washed, dehydrated in graded ethanol, saturated with xylene and embedded in paraffin. Histological analysis of the paraffin sections were carried out, such as hematoxylin and eosin (HE) staining and Masson's trichrome staining.

Statistical Analysis. AO II, TBO test, all blood and cell assay were carried out at least three times with more than four parallel samples. The dates were offered as mean ± standard deviation (SD). Statistical analysis were completed using one-way analysis of variance (ANOVA), with $*p < 0.05$ suggesting significant difference.

3. RESULTS AND DISCUSSION

Grazing incidence attenuated total reflection Fourier transform infrared spectroscopy (GATR-FTIR) was performed to analyze the chemical structures of PDAM, PDAM/HD and Hep-PDAM/HD (see Figure S1 in the Supporting Information). Except the basic features of the chemical structure of the PDAM coating, there were some obvious differences in the C−H and N−H peaks observed on PDAM/HD. It is noteworthy that there was a considerably reinforcement of the peaks that relate to the stretching vibrations of ν−N−H (−NH_2) at 3340 and 3270 cm^{-1} and deformation vibrations of γ (NH) at 700 cm^{-1}, suggesting the presence of copolymerization reaction of dopamine with HD as well as a good retention of −NH_2 of HD. In the spectrum of the Hep-PDAM/HD, the characteristic heparin peaks could be observed at 1235 and 3490 cm^{-1}, ascribed to S═O bond and −COOH, respectively. Note that the remarkable reinforced peak of amide I and II (−CONH) at 1668 and 1565 cm^{-1} in Hep-PDAM/HD spectrum revealed the condensation reaction between the −COOH and −NH_2. XPS analysis also showed a significant difference in the chemical compositions between PDAM and PDAM/HD. The addition of HD clearly altered the surface chemical compositions of the coatings, as seen in a significant increase in the nitrogen content, and a decay in the contents of carbon and oxygen of the PDAM/HD (see Table S1 in the Supporting Information). Matrix-assisted laser desorption ionization time-of-flight mass spectrometry (MALDI-TOF MS) analyses were performed for further understanding of the possible polymerization process (see Figure S2 in the Supporting Information). Before the analysis of polymerization mechanism of the PDAM/HD, the analysis of the MALDI-TOF MS spectrum of PDAM was first carried out. The recent studies showed that the PDAM formation was associated with a complex polymer structure and the mechanism of buildup. Vecchia et al.[37] found that PDAM consists of three main building blocks, uncyclized catecholamine/quinones, cyclized 5,6-dihy-droxyindole (DHI) units, and pyrrolecarboxylic acid moieties. Hong et al.[38] have reported that a variety of possible intermolecular interactions such as ionic, cation−π, π−π, quadrupole−quadrupole, and hydrogen bonding (H-bonding) interactions contributed to the physical self-assembly pathway to PDAM formation. Our result of MALDI-TOF MS spectrum of PDAM (see Figure S2A, C in the Supporting Information) also confirmed such a polymerization mechanism, and the incorporation of Tris into PDAM was also demonstrated by the detection of the peaks at 409, 391, and 273 m/z. For the PDAM/HD synthesis, the introduction of HD significantly influenced the self-polymerization manner of dopamine (see Figure S2B, D in the Supporting Information), the incorporation of HD into PDAM was mainly based on Michael addition and Schiff base chemistries, as well as the electrostatic interaction of −NH_3^+ of HD and O− of Tris or dopamine (this can be evidenced by the presence of the peak of −NH_3^+ around 401.7 eV shown in Figure S3 in the Supporting Information). Additionally, an AO II test showed that the amine group density of PDAM/HD coating was 30 nmol/cm^2. The thickness was 140 nm determined by ellipsometry.

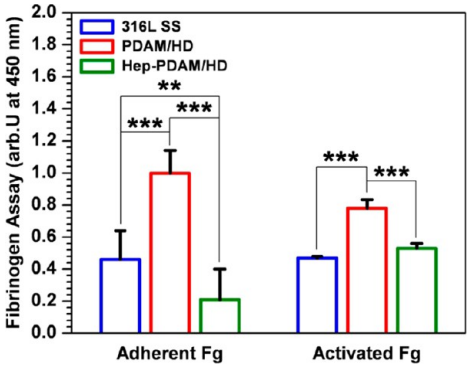

Figure 2. Relative amounts of adsorbed fibrinogen and exposure of γ chain on 316L SS, PDAM/HD and Hep-PDAM/HD. Data presented as mean ± SD and analyzed using a one-way ANOVA, $**p < 0.01$, $***p < 0.001$.

Heparin was covalently immobilized on PDAM/HD coating using carbodiimide coupling chemistry. XPS analysis revealed a clear S 2p signal (Figure 1A, B), confirming the successful immobilization of heparin on the PDAM/HD surface. The conjugation of heparin significantly changed the chemical composition of the surface by a remarkable decrease in carbon content and increase in oxygen and sulfur content (see Table S1 in the Supporting Information). Furthermore, the appearance of the new peaks of −$NHSO_3^-$ at 401.3 eV (see Figure S3 in the Supporting Information) and OSO_3^- at 532 eV (Figure 1C) also provided evidence of the successful immobilization of heparin onto the PDAM/HD coating. The density of heparin grafted on the coating plays a substantial role in selectively directing the behaviors of platelet and vascular cells.[15] Thus, TBO test was further performed to determine the

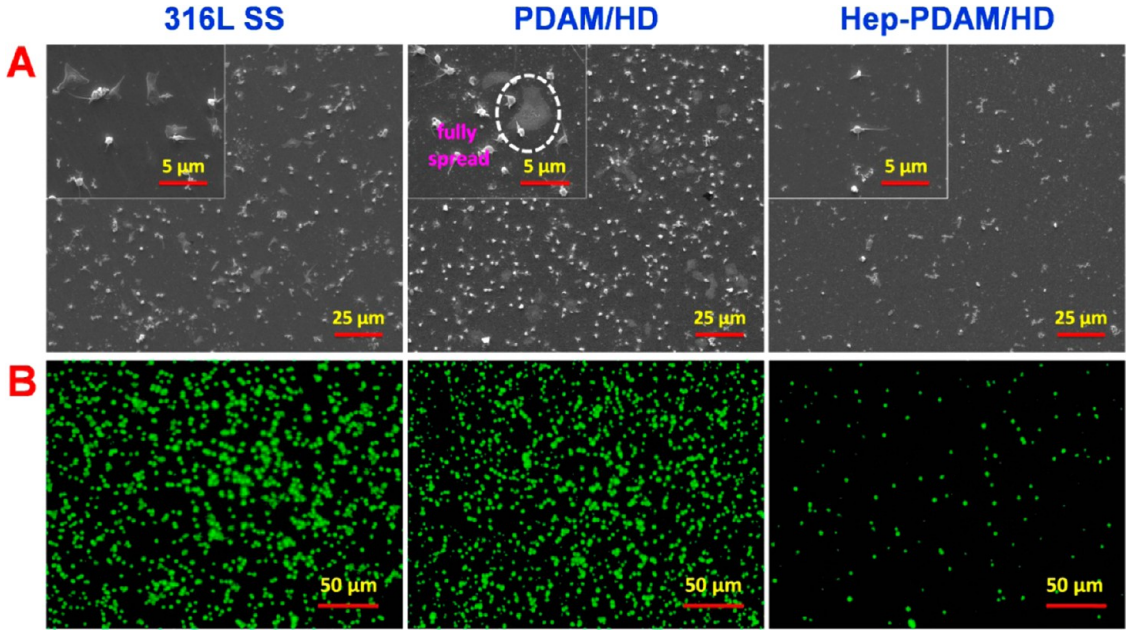

Figure 3. (A) Representative SEM images of platelets adherent on 316L SS, and the PDAM/HD coating before and after heparin conjugation; (B) representative images of P-selectin staining, showing activated platelets labeled with a green fluorescent dye.

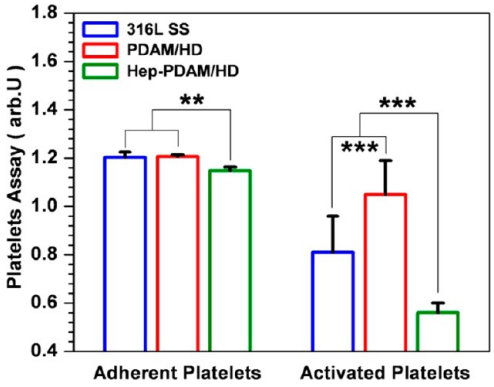

Figure 4. Relative amount of adherent platelets (results gained by LDH assay) and activated platelets (results gained by GMP-140 assay) on 316L SS, PDAM/HD and Hep-PDAM/HD. Data presented as mean ± SD and analyzed using a one-way ANOVA, $^{**}p < 0.01$, $^{***}p < 0.001$.

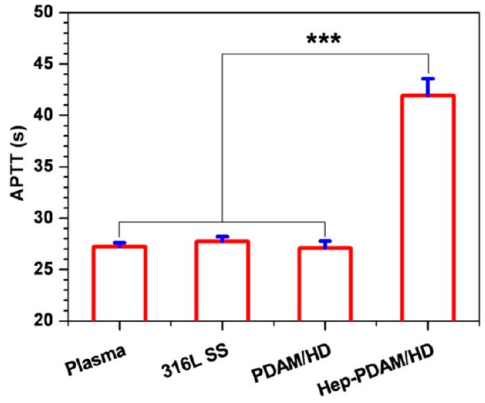

Figure 5. APTTs of native plasma, and plasma after incubation with 316L SS and PDAM/HD coating before and after heparin conjugation. Data presented as mean ± SD and analyzed using a one-way ANOVA, $^{***}p < 0.001$.

amount of heparin bound to the PDAM/HD surface. The result showed that approximate 900 ng/cm^2 of heparin was introduced to the PDAM/HD coating.

The stability of heparin is important for the safe performance and sufficient anticoagulation of vascular stents or grafts decorated with heparin. Nuner et al.[39] demonstrated that local heparin delivery could inhibit thrombus formation at a heparin amount that is several orders of magnitude lower than required as systemic dose, and local delivery of heparin is not related to the prolongation of bleeding parameters. Herein, robust heparin binding should be safe in clinical use. Covalent immobilization improves the stability and persistence, and it avoids the burst release of the immobilized biomolecules compared to physical and electrostatic adsorption.[32] Figure 1D exhibits the relative amount of heparin retained on Hep-PDAM/HD surfaces after immersion into PBS for various periods of time (presented by sulfur atomic %, rated to 0 day as 100%). After continuous immersion in PBS for 30 days, the Hep-PDAM/HD retained about 80% of the S content, indicating an excellent stability of heparin, and suggesting the potential for application in long-term implanted vascular devices.

For blood-contacting materials, hemocompatibility is the leading requirement in directing the design of vascular devices. As blood is the first body fluid come into contact with implants after implantation into the blood vessel, special attention must be paid to the behavior of blood components. A blood-contacting material with ideal hemocompatibility should not induce any activation or denaturation of blood components.

Plasma proteins have the tendency to adsorb quickly onto a material surface and subsequently mediate platelet adhesion and trigger blood coagulation, leading to thrombus formation.[40] The amount and conformational change of adsorbed Fg, i.e., exposure of the γ chain (HHLGGAKQAGDV at γ 400−411),[41] plays a key role in the interactions between platelets and materials. As shown in Figure 2, there was much more Fg adsorbed on PDAM/HD surface compared to 316 L SS. This may due to the amine-rich surface with less negative charges.

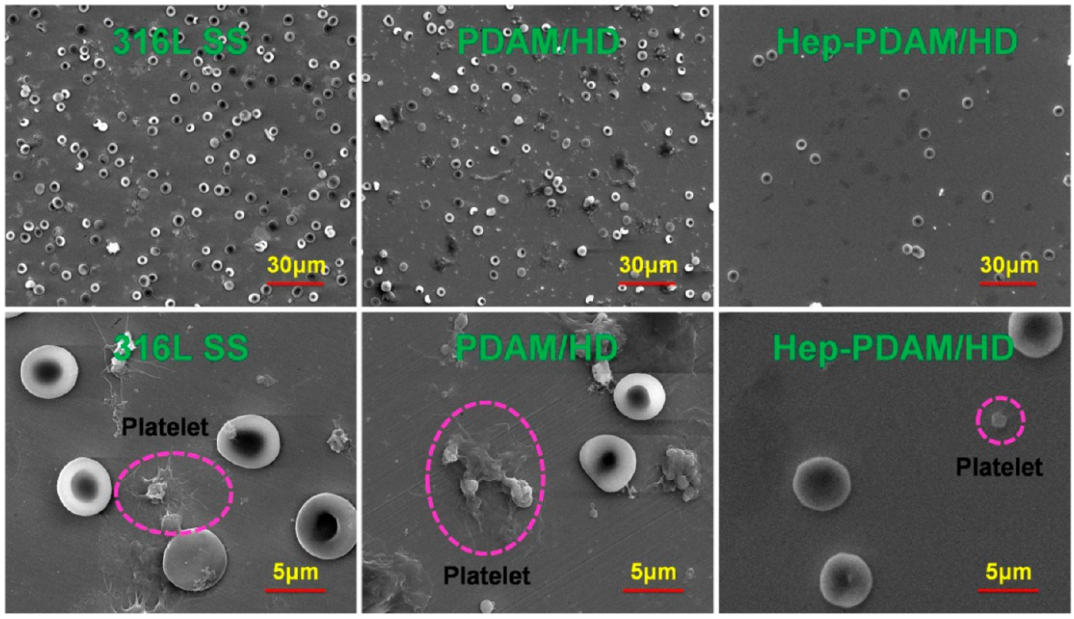

Figure 6. Representative SEM images of 316L SS and the PDAM/HD coating before and after heparin conjugation after incubation in a modified Chandler loop with whole blood for 2 h.

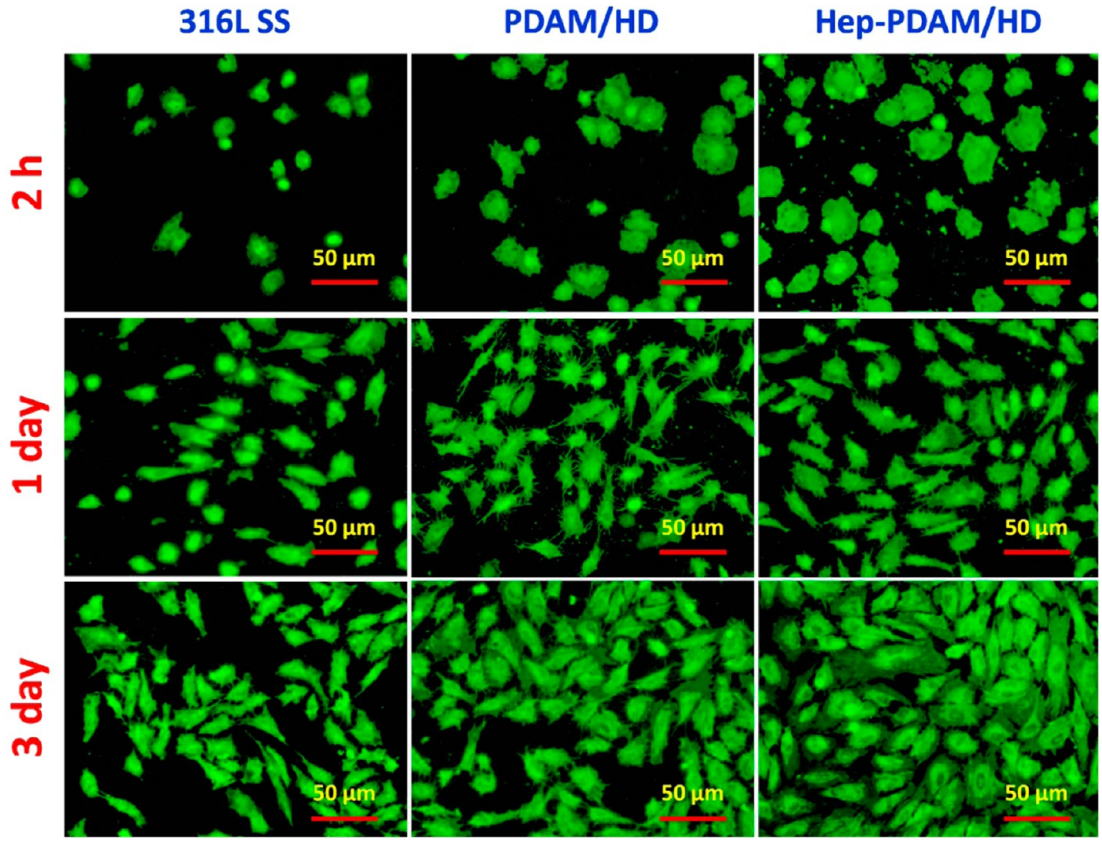

Figure 7. Rhodamine123 fluorescence staining of HUVECs cultured on the 316L SS, PDAM/HD, and Hep-PDAM/HD surfaces after culture of 1 and 3 days.

Additionally, the chemical interactions between PDAM/HD and Fg may also lead to more Fg adsorption.[42−44] However, the introduction of heparin significantly decreased the Fg adsorption. This indicates that Hep-PDAM/HD resists Fg adsorption, and this already contributes to an improved hemocompatibility. It has been demonstrated that the exposure of γ chain sequences allowes Fg to bind to the GPIIb/IIIa integrin receptor on the platelet membrane.[45] The denaturation of Fg is considered to be more important for platelet adhesion and thrombus formation than the absolute amount of adsorbed Fg.[46,47] As shown in Figure 2, the PDAM/HD coating on 316 L SS stimulated Fg activation. This may be attributed to the

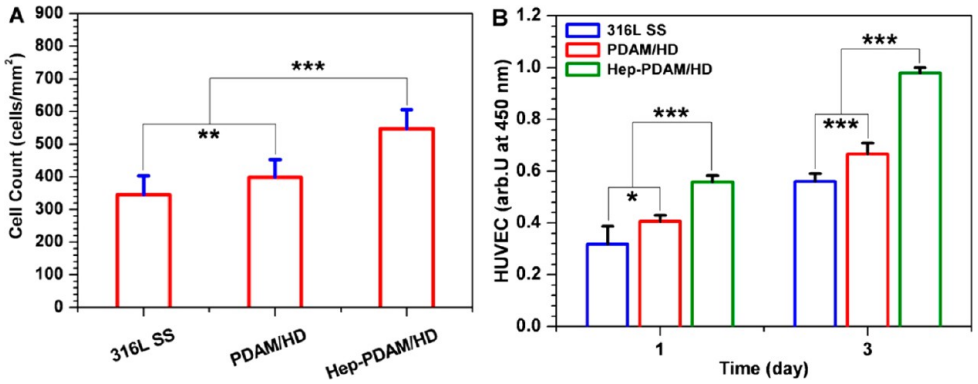

Figure 8. (A) Amounts of HUVECs attached onto the 316L SS, PDAM/HD, and Hep-PDAM/HD surfaces after 2 h culture, calculated from at least 12 images; (B) proliferation of HUVECs cultured on the 316L SS, PDAM/HD and Hep-PDAM/HD surfaces after 1 and 3 days culture (using CCK-8 kit). Data presented as mean ± SD and analyzed using a one-way ANOVA, $*p < 0.05$, $**p < 0.01$, $***p < 0.001$.

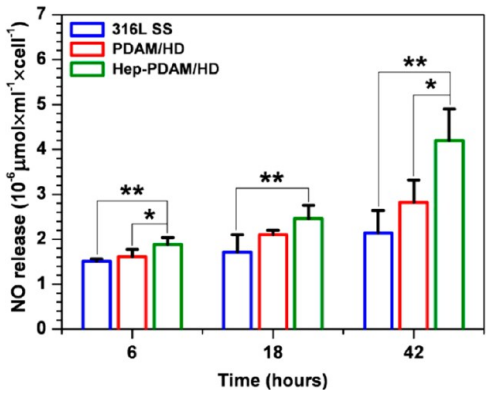

Figure 9. NO levels released to the culture media for the 316L SS, PDAM/HD, and Hep-PDAM/HD (size of the samples: Φ18 mm, $n = 4$). Data presented as mean ± SD and analyzed using a one-way ANOVA, $*p < 0.05$, $**p < 0.01$, $***p < 0.001$.

positively charged PDAM/HD coating due to its amine-rich groups and the highly negatively charged Hep-PDAM/HD, which may either accelerate or prevent proteins on the materials surface from denaturation by accelerating or preventing charge transfer from the protein into the material.[48] However, the conjugation of heparin to the PDAM/HD surface resulted in a significantly suppressed exposure of γ chain of Fg.

Adhesion and activation levels of platelets are essential parameters in the evaluation of the hemocompatibility of biomaterials. The activation level of adherent platelets is closely connected with their morphology, with five classic stages defined as round, dendritic, spreading dendritic, spreading and fully spreading in correlation with increased activated levels.[49] Figure 3A shows SEM images of platelets adherent on the different samples. Clearly, most platelets aggregated on 316 L SS and exhibited spreading dendritic and spreading stages. The deposition of PDAM/HD further trigger platelet activation, large amount of spreading even fully spreading platelets were present. In contrast, on the Hep-PDAM/HD surface, only a small number of platelets was observed. These significant differences were further confirmed by the P-selectin stain (Figure 3B). P-selectin, a 140-kDa granule integral membrane glycoprotein also called GMP-140, which belongs to the selectin family, can be up-regulated by a factor of 10 on the surface membrane of activated platelets.[50,51] As P-selectin is highly related to platelet activation, the decreased amount on the Hep-PDAM/HD surface indicated good hemocompatibility.

Adhesion density and activity of the platelets was further quantified by LDH and P-selectin assay, respectively. As shown in Figure 4, the Hep-PDAM/HD coating exhibited significant inhibition in platelet adhesion compared to both 316 L SS and PDAM/HD. In agreement with P-selectin visualization (Figure 3B), PDAM/HD up-regulated the expression of GMP-140 compared to 316 L SS, but after heparin conjugation, the GMP-140 expression was substantially reduced, demonstrating a significant inhibition of the platelet activation. The obvious lower P-selectin expression of platelets on the Hep-PDAM/HD surface promises less platelet aggregation and less platelet clot formation.

APTT test was performed to measure the potency of the samples in delaying coagulation through the intrinsic coagulation mechanism. It is well-known that heparin exerts its anticoagulant properties by binding to ATIII specifically and inactivating the clotting Factors IXa, Xa, and IIa. As shown in Figure 5, there was no significant difference in the APTT among the control plasma, 316L SS and PDAM/HD. However, the conjugation of heparin to PDAM/HD remarkably prolonged the APTT for about 15s.

In this work, a whole blood assay was carried out under flow condition to synthetically evaluate the thrombogenicity of the 316L SS, PDAM/HD and Hep-PDAM/HD. As shown in Figure 6, there was severe platelet activation and red blood cell aggregation on both 316L SS and PDAM/HD surfaces. As expected, with the minimal activation of platelets or plasma coagulation cascade even under flow conditions, the Hep-PDAM/HD coating exhibited hemocompatibility surpassed the clinical standard SS.

A native intact endothelium as the inner lining of the blood vessels is fundamental to maintain cardiovascular homeostasis and has a tight control over SMCs proliferation and platelets activity. The potential to regenerate healthy endothelium plays a key role in determining success or failure of a stent coating *in vivo*. Promoted attachment, spreading, proliferation, migration, and function of EC are crucial factors for complete endothelialization. Thus, the growth behavior of ECs on Hep-PDAM/HD was systematically evaluated.

Generally speaking, mammalian cells experience a cell adhesion process consisting of cell attachment, spreading, cytoskeleton organization, and development of focal adhesion.[52] In this work, cell attachment was first explored as the

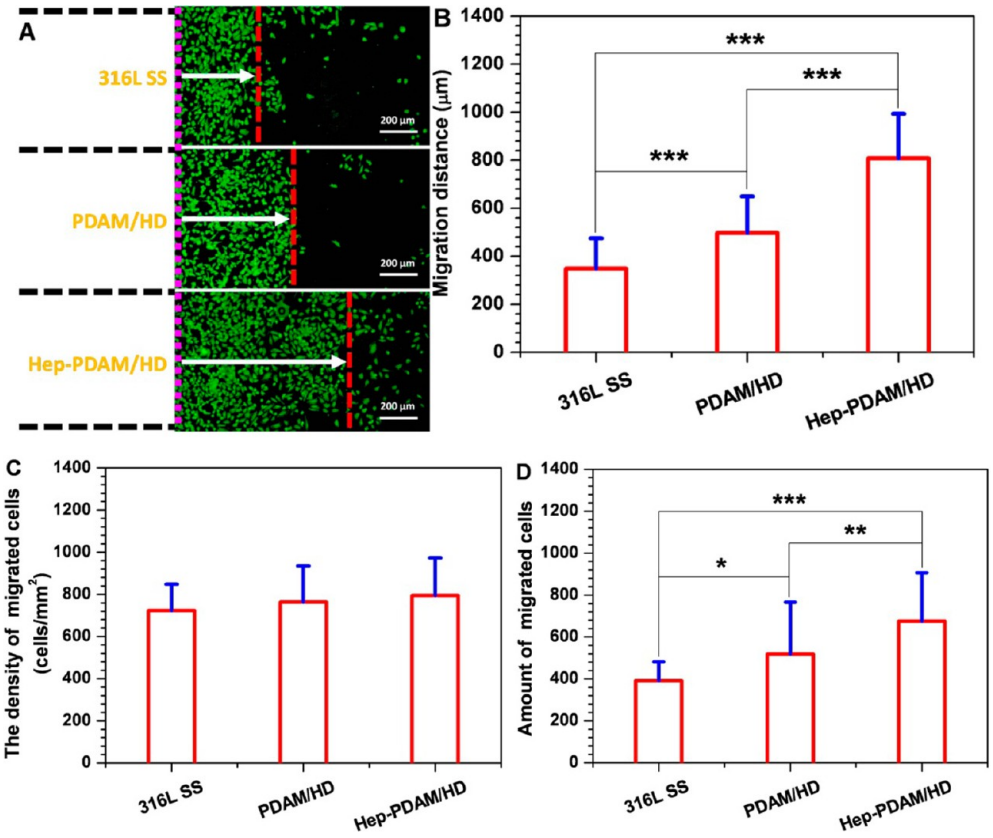

Figure 10. (A) Migration and (B) migration distance, (C) density of migrating cells, and (D) amount of migrating HUVECs on the 316L SS, PDAM/HD, and Hep-PDAM/HD surfaces after 1 day culture. The data were calculated from at least 12 images. Data presented as mean ± SD and analyzed using a one−-way ANOVA, *$p < 0.05$, **$p < 0.01$, ***$p < 0.001$.

interaction between cells and substrates. A 2 h short-time culture of HUVECs revealed that the PDAM/HD coating provided a better microenvironment to support EC attachment and spreading compared to 316L SS (Figure 7), as evidenced by a significant increase of about 15.4% in the number of adherent cells (Figure 8A) and of about 78.7% in the projected area per cell (see Figure S4A in the Supporting Information). The immobilization of the heparin on the PDAM/HD coating resulted in a further enhancement in cell attachment and spreading, with an increase of 37.4% in the number of adherent cells and 18.1% in the projected area per cell.

The fluorescence microscopy revealed the best cytoskeleton development of HUVECs grown on the Hep-PDAM/HD coating (Figure 7). After 1 day's culture, the cells grown on Hep-PDAM/HD had a remarkably larger projected area (see Figure S4A in the Supporting Information) and lower minor/major axis ratio (see Figure S4B in the Supporting Information) than 316 L SS and PDAM/HD, which present accelerated cell spreading and cytoskeleton stretching. While the projected area of cells grown on PDAM/HD and Hep-PDAM/HD coating increased with the extension of culture time, the shape index (0 for a straight line and 1 for perfectly round) of cells on Hep-PDAM/HD remained lower than on 316 L SS (see Figure S4B in the Supporting Information), revealing the better cell function.[53]

Furthermore, the proliferation of HUVECs cultured on the Hep-PDAM/HD was greatly faster than on either the 316L SS or the PDAM/HD (Figure 8B). The above data indicate that the HUVECs on the Hep-PDAM/HD followed the aforementioned general adhesion processes of substrate attachment, spreading, and cytoskeleton development and then proliferation in a well-defined way.

Healthy ECs in native blood vessels can inhibit platelet activation and aggregation, regulate vasodilation and suppress SMC proliferation by producing NO continuously.[54,55] It is of great importance to maintain the special function of releasing NO of the adherent ECs on Hep-PDAM/HD. Herein, the NO release per cell was determined to evaluate the EC function. As shown in Figure 9, the PDAM/HD coating promoted the release of NO compared to 316L SS, whereas Hep-PDAM/HD further enhanced the NO production.

The migration of healthy ECs into the damaged vessel area is a key approach of endothelium regeneration. As reported, the elongated cells could not only improve proliferation and extracellular matrix production, but also possess higher migration speed.[53,56] As shown in Figure 10, the migration distance and number of migrated cells on PDAM/HD coating were much larger than that on 316 L SS. After heparin immobilization, there was a significantly enhanced migration distance and increased amount of migrating ECs, which confirmed the deduction for the analysis of cell morphology.

These results indicated that the Hep-PDAM/HD coating improves the attachment, spreading, proliferation and migration behavior as well as promotes the release of NO, suggesting a promising potential for accelerating the re-endothelialization process on a stent.

The interactions between heparin and various growth factors (such as, VEFG, EGF) consequently offer the possibility of promoted endothelialization. Gong et al.[57] reported that after implantation of heparin coated stents in porcine coronary

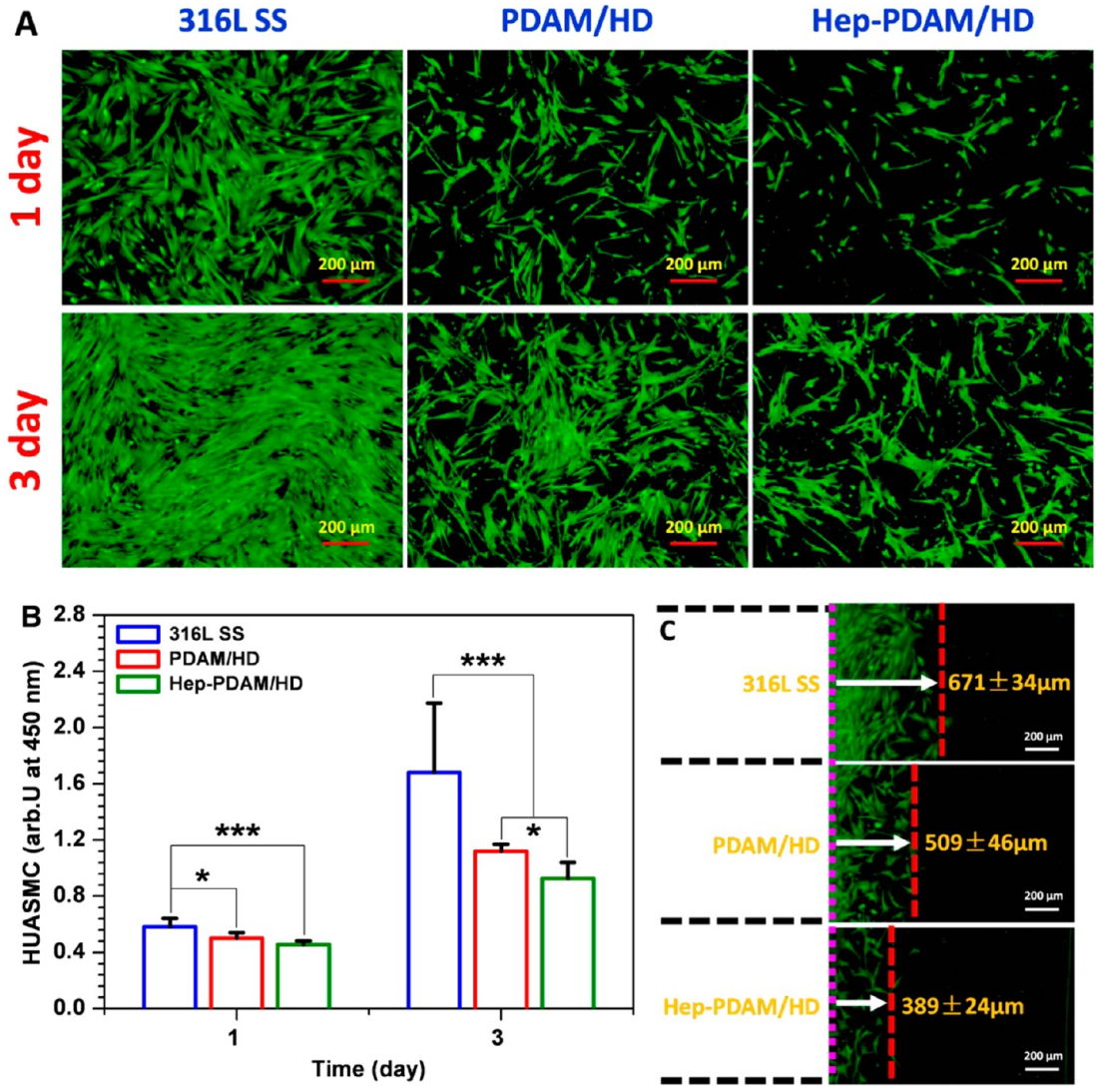

Figure 11. (A) Rhodamine123 fluorescence staining and (B) proliferation of HUASMCs on the 316L SS, PDAM/HDm and Hep-PDAM/HD surfaces after culture of 1 and 3 days. (C) Migration of HUASMCs on the 316L SS, PDAM/HD, and Hep-PDAM/HD surfaces after 1 day culture. Data presented as mean ± SD and analyzed using a one-way ANOVA, $*p < 0.05$, $***p < 0.001$.

arteries for 1 month, the surface with 2.6 $\mu g/cm^2$ heparin density was fully covered by ECs, whereas the 6.3 $\mu g/cm^2$ heparin surface was only incompletely covered. In our previous study, we found that a surface with low heparin density down to ~3.5 $\mu g/cm^2$ selectively inhibits SMC proliferation but promote EC growth.[27,30] In this work, the conjugated heparin density was ~900 ng/cm^2, which also exhibited enhanced ECs growth.

The stent implantation process is associated with acute vessel wall injury which induces pathological complications, hence triggers VSMC proliferation resulting in in-stent restenosis (ISR).[58,59] Inhibition of VSCM proliferation is the key challenge for the prevention of ISR. In addition to the well-known anticoagulant function, heparin is known to show a remarkable antiproliferative effect on VSMCs, further, it is an effective modulator to induce the expression of contractile SMC phenotype markers.[22,60,61] In this work, the HUASMC growth behavior was evaluated. The Hep-PDAM/HD coating significantly reduced cell adhesion after 2 h, with 67.2 and 75% decrease compared to 316 L SS and PDAM/HD coating (see Figure S5 in the Supporting Information). The analysis for the morphology (Figure 11A) and proliferation (Figure 11B) of HUASMCs revealed that the Hep-PDAM/HD coating effectively inhibited cell adhesion and proliferation. It was noteworthy that the migration behavior of HUASMCs on Hep-PDAM/HD surface was remarkably reduced (Figure 11C), manifested in both the migration distances and the density of the migrated cells. These results suggest that the Hep-PDAM/HD coating may help to mitigate restenosis.

Since the function of a healthy and intact endothelium in the prevention and reduction of restenosis and thrombosis has been highlighted, numerous strategies have been developed to accelerate endothelialization.[62,63] However, most strategies focused on only enhancing ECs growth, while ignoring antiproliferative and anticoagulant properties.[64] These efforts might be misleading and meaningless *in vivo*. For instance, the recently developed anti-CD34 antibody coated stent (Genous Bioengineered R stent, Orbus Medical Technologies) has shown rapid endothelialization after implantation in clinical trials. However, long-term studies revealed that the antirestenosis effects were not as remarkable as expected, and there was no significant reduction in neointimal hyperplasia compared

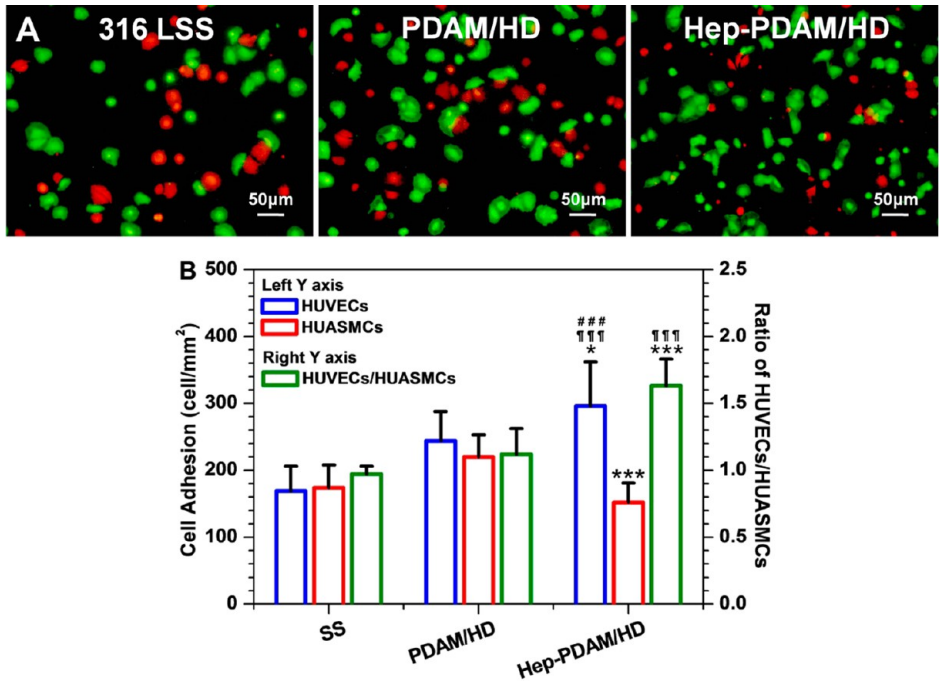

Figure 12. (A) CMFDA-labeled HUVECs (green) and CMTMR-labeled HUASMCs (orange) after 2 h coculture on the 316L SS, PDAM/HD, and Hep-PDAM/HD surfaces. (B) Left Y axis shows the amount of cells adherent on the surface and the right Y axis shows the ratio of HUVECs/HUASMCs, determined from at least six images. Data presented as mean ± SD and analyzed using a one-way ANOVA, $^{*}p < 0.05$, $^{***}p < 0.001$ (Hep-PDAM/HD vs PDAM/HD), $^{¶¶¶}p < 0.001$ (Hep-PDAM/HD vs 316L SS), $^{###}p < 0.001$ (HUVECs vs HUASMCs).

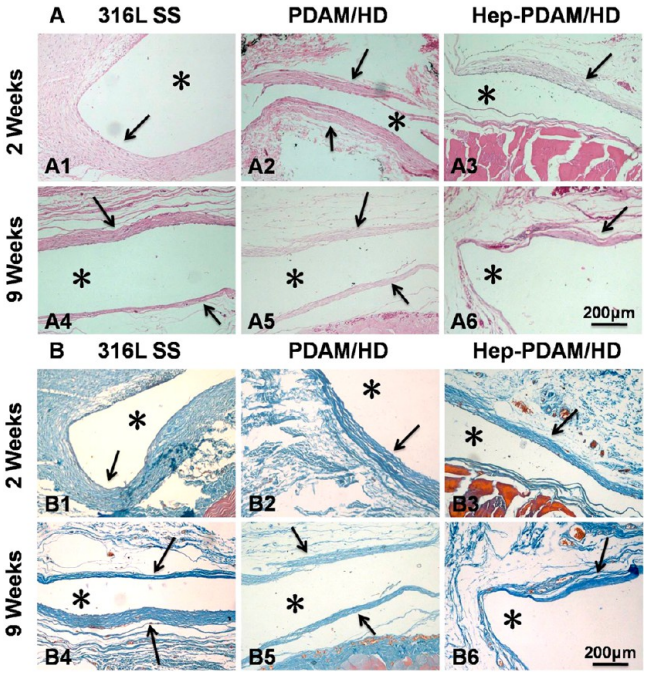

Figure 13. (A) HE and Masson's (B) trichrome stainings of subcutaneous tissues around bare and PDAM/HD, Hep-PDAM/HD coated 316L SS implants after 2 and 9 weeks implantation, respectively. * Represents the implant site.

with the conventional bare metal stent implantation.[64] Insufficient specifity of the anti-CD34 antibody for EPCs has been considered to be the major reason. The handicap of EPCs in the competitive growth with SMCs at stent implantation site was ignored. SMCs in atherosclerosis and in culture mainly have a proliferating and synthetic phenotype. A confluent and adherent layer of endothelium can be cultured on quiescent SMCs but not on synthetic SMCs.[65] Thus, special attention should be paid not only to rapid endothelialization of the stent, but also to consider the competitive growth between ECs and SMCs and the influence of SMCs phenotype.

Therefore, a coculture assay was further carried out to test the competitive attachment and growth of HUVECs and HUASMCs.[35] Cell trackers were used to label the cells before cultivation, HUVECs were marked green and HUASMCs orange, respectively. The fluorescence micrographs and number of the adherent cells after 2 h are shown in Figure 12A, B. The amount of HUVECs and HUASMCs adherent on 316 L SS was almost equivalent. Although there were considerably higher amounts of both cells on the PDAM/HD coating, the ratio of HUVECs to HUASMCs was enhanced. After heparin conjugation, the amount of adherent HUVECs was dramatically enhanced, while the amount of HUASMCs was remarkably reduced, showing competitive adhesion advantage of HUVECs over HUASMCs with significantly increased ratio of HUVECs/HUASMCs. Additionally, the Hep-PDAM/HD coating significantly enhanced HUVECs growth and remarkably inhibited HUASMCs growth after 1 day culture compared to 316L SS and PDAM/HD coating (see Figure S6 in the Supporting Information).

Atherosclerosis is a chronic inflammation in arteries, characterized by a large amount of lipid deposition onto blood vessel walls, a variety of inflammatory cells (such as macrophages, lymphocytes and neutrophils) infiltration and SMCs hyperplasia. It has also been demonstrated that both local and systemic inflammation promote neointimal proliferation through the stent struts and play a pivotal role in the pathogenesis of ISR.[1] A complex series of inflammatory events modulated by several types of inflammatory cells are involved in the tissue responses to implanted biomaterials. Meanwhile,

tissue response may impair the safety, function and performance of implanted medical devices via interaction with biological components.[66,67] Thus, lighter tissue response is expected as a valuable characteristic of vascular stent coatings.

The tissue response to Hep-PDAM/HD coating was evaluated by subcutaneous implantation in rabbits for different periods of time. Then a quantitative histological analysis was carried out (Figure 13). Bare 316L SS, PDAM/HD, and Hep-PDAM/HD-coated 316L SS did not induce local toxic effects and obvious local tissue reactions. For control 316L SS, much granulation and a thick fibrous capsule (185 ± 34 μm) were observed, indicating a slight inflammatory response (Figure 13A1 and B1). The introduction of PDAM/HD coating attenuated the granulation response and fibrous capsule formation (109 ± 22 μm) (Figure 13A2 and B2). For Hep-PDAM/HD coated 316L SS, there was even less granulation and a thinner fibrous capsule (83 ± 20 μm) formed at the tissue/material interface (Figure 13A3 and B3). Fibrous encapsulation often separates the implanted foreign body from normal host tissue sites. Dense and frequently poorly vascularized capsules may compromise the performance of the implanted medical devices (e.g., vascular stents) and pose a risk of infection for the implanted site. The thicker fibrous encapsulation implies more serious tissue response.[66,68] For 9 weeks' implantation, no significant difference in fibrous encapsulation was observed between the control 316L SS (76 ± 11 μm), PDAM/HD (74 ± 8 μm), and Hep-PDAM/HD (71 ± 10 μm) coated 316L SS (Figure 13A3, A4, A5 and B3, B4, B5). Overall, the introduction of Hep-PDAM/HD coating had mitigated tissue response around the implantation site, suggesting an excellent and acceptable application in surface modification of vascular stents for demanding long-term performance.

4. CONCLUSION

We presented a facile method to prepare a multifunctional coating through covalent immobilization of heparin onto a PDAM/HD coating, which is rich in amine groups. The Hep-PDAM/HD coating not only showed remarkable improvement in hemocompatibility but also considerable enhancement in HUVEC adhesion, proliferation, migration, and NO release, whereas there was substantial inhibition in HUASMCs adhesion and proliferation. Moreover, the coating provided a beneficial platform for competitive adhesion in HUVECs over HUASMCs. It is worth mentioning that the Hep-PDAM/HD coating also exhibited excellent tissue compatibility, which is one of the most valuable characteristics of stent coating. These results suggest a promising potential of the Hep-PDAM/HD coating to avoid vascular stent associated complications. Thus, the considerations into how Hep-PDAM/HD coating interacts with vascular tissue *in vivo* will be covered in future work.

■ ASSOCIATED CONTENT

Supporting Information

Figure S1 for the GATR-FTIR spectra of the PDAM, PDAM/HD, and Hep-PDAM/HD coatings. Figure S2 for the MALDI-TOF MS spectrum of the PDAM and PDAM/HD coating, with tentative structures assigned to main peaks. Table S1 for the atomic compositions of the PDAM/HD coating before and after heparin conjugation obtained by XPS. Figure S3 for the high-resolution N 1s XPS spectra of the PDAM/HD and Hep-DAM/HD coatings. Figure S4 for the projected area per cell and Minor/major axis ratio of cells (HUVECs were cultured on the 316L SS, PDAM/HD and Hep-PDAM/HD for 2, 24, and 72 h). Figure S5 for the amounts of HUASMCs attached after 2 h. Figure S6 for CMFDA labeled HUVECs (green) and CMTMR labeled HUASMCs (orange) after 1 day coculture on the 316L SS, PDAM/HD and Hep-PDAM/HD surfaces. This material is available free of charge via the Internet at http://pubs.acs.org/.

■ AUTHOR INFORMATION

Corresponding Authors

*E-mail: zhiluyang1029@126.com. Tel: +86 28 87600625. Fax: +86 28 87600625.
*E-mail: nhuang@263.net

Notes

The authors declare no competing financial interest.

■ ACKNOWLEDGMENTS

This work was supported by the NSFC (Project 81271701 and 51173149), the Ministry of Science and Technology of China (Key Basic Research Project No. 2011CB606204), and NSFC Key Program 81330031.

■ REFERENCES

(1) Ward, M. R.; Stewart, D. J.; Kutryk, M. J. Endothelial Progenitor Cell Therapy for the Treatment of Coronary Disease, Acute MI, and Pulmonary Arterial Hypertension: Current Perspectives. *Catheter Cardiovasc. Intervention* **2007**, *70*, 983−998.
(2) Zilberman, M.; Eberhart, R. C. Drug-Eluting Bioresorbable Stents for Various Applications. *Annu. Rev. Biomed. Eng.* **2006**, *8*, 153−180.
(3) Eisenberg, M. J.; Konnyu, K. J. Review of Randomized Clinical Trials of Drug-Eluting Stents for the Prevention of in-stent Restenosis. *Am. J. Cardiol.* **2006**, *98*, 375−382.
(4) Colombo, A.; Drzewiecki, J.; Banning, A.; Grube, E.; Hauptmann, K.; Silber, S. Randomized Study to Assess the Effectiveness of Slow- and Moderate-Release Polymer-Based Paclitaxel-Eluting Stents for Coronary Artery Lesions. *Circulation* **2003**, *108*, 788−794.
(5) Achneck, H. E.; Sileshi, B.; Parikh, A.; Milano, C. A.; Welsby, I. J.; Lawson, J. H. Pathophysiology of Bleeding and Clotting in the Cardiac Surgery Patient: From Vascular Endothelium to Circulatory Assist Device Surface. *Circulation* **2010**, *122*, 2068−2077.
(6) McGuigan, A. P.; Sefton, M. V. The Influence of Biomaterials on Endothelial Cell Thrombogenicity. *Biomaterials* **2007**, *28*, 2547−2571.
(7) Avci-Adali, M.; Paul, A.; Ziemer, G.; Wendel, H. P. New Strategies for *in vivo* Tissue Engineering by Mimicry of Homing Factors for Self-Endothelialisation of Blood Contacting Materials. *Biomaterials* **2008**, *29*, 3936−3945.
(8) Brewster, L. P.; Brey, E. M.; Greisler, H. P. Cardiovascular Gene Delivery: the Good Road is Awaiting. *Adv. Drug. Delivery Rev.* **2006**, *58*, 604−629.
(9) Peyton, S. R.; Kim, P. D.; Ghajar, C. M.; Seliktar, D.; Putnam, A. J. The Effects of Matrix Stiffness and RhoA on the Phenotypic Plasticity of Smooth Muscle Cells in a 3-D Biosynthetic Hydrogel System. *Biomaterials* **2008**, *29*, 2597−2607.
(10) Capila, I.; Linhardt, R. J. Heparin-Protein Interactions. *Angew. Chem., Int. Ed.* **2002**, *41*, 390−412.
(11) Rabenstein, D. L. Heparin and Heparan Sulfate: Structure and Function. *Nat. Prod. Rep.* **2002**, *19*, 312−331.
(12) Bjork, I.; Lindahl, U. Mechanism of the Anticoagulant Action of Heparin. *Mol. Cell. Biochem.* **1982**, *48*, 161−182.
(13) Boyle, J. P.; Smart, R. H.; Shirey, J. K. Heparin in the Treatment of Chronic Obstructive Bronchopulmonary Disease. *Am. J. Cardiol.* **1964**, *14*, 25−28.
(14) Fine, N. L.; Shim, C.; Williams, M. H. Objective Evaluation of Heparin in the Treatment of Asthma. *Am. Rev. Respir. Dis.* **1968**, *98*, 886−887.

(15) Liu, T.; Liu, Y.; Chen, Y.; Liu, S. H.; Maitz, M. F.; Wang, X.; Zhang, K.; Wang, J.; Wang, Y.; Chen, J. Y.; Huang, N. Immobilization of Heparin/Poly-L-lysine Nanoparticles on Dopamine-Coated Surface to Create a Heparin Density Gradient for Selective Direction of Platelet and Vascular Cells Behavior. *Acta Biomater.* **2014**, *10*, 1940−1954.
(16) Li, G. C.; Yang, P.; Liao, Y. Z.; Huang, N. Tailoring of the Titanium Surface by Immobilization of Heparin/Fibronectin Complexes for Improving Blood Compatibility and Endothelialization: an *in vitro* Study. *Biomacromolecules* **2011**, *12*, 1155−1168.
(17) Sakiyama-Elbert, S. E. Incorporation of Heparin into Biomaterials. *Acta. Biomater.* **2014**, *10*, 1581−1587.
(18) Cardin, A. D.; Jackson, R. L.; Sparrow, D. A.; Sparrow, J. T. Interaction of Glycosaminoglycans with Lipoproteins. *Ann. N.Y. Acad. Sci.* **1989**, *556*, 186−193.
(19) Sangaj, N.; Kyriakakis, P.; Yang, D.; Chang, C. W.; Arya, G.; Varghese, S. Heparin Mimicking Polymer Promotes Myogenic Differentiation of Muscle Progenitor Cells. *Biomacromolecules* **2010**, *11*, 3294−3300.
(20) Zhang, L.; Furst, E. M.; Kiick, K. L. Manipulation of Hydrogel Assembly and Growth Factor Delivery *via* the Use of Peptide−Polysaccharide Interactions. *J. Controlled Release* **2006**, *114*, 130−142.
(21) Maitz, M. F.; Freudenberg, U.; Tsurkan, M. V.; Fischer M.; Beyrich, T.; Werner, C. Bio-Responsive Polymer Hydrogels Homeostatically Regulate Blood Coagulation. *Nat. Commun.* **2013**, *4*, DOI: 10.1038/ncomms3168.
(22) Clowes, A. E.; Karnowsky, M. J. Suppression by Heparin of Smooth Muscle Cell Proliferation in Injured Arteries. *Nature* **1977**, *265*, 625−626.
(23) Ahn, Y. K.; Jeong, M. H.; Kim, J. W.; Kim, S. H.; Cho, J. H.; Cho, J. G. Preventive Effects of the Heparin-Coated Stent on Restenosis in the Porcine Model. *Catheter Cardiovasc. Intervention* **1999**, *48*, 324−330.
(24) Cariou, R.; Harousseau, J. L.; Tobelem, G. Inhibition of Human Endothelial Cell Proliferation by Heparin and Steroids. *Cell. Biol. Int. Rep.* **1988**, *12*, 1037−1047.
(25) Khorana, A. A.; Sahni, A.; Altland, O. D.; Francis, C. W. Heparin Inhibition of Endothelial Cell Proliferation and Organization is Dependent on Molecular Weight. *Arterioscler. Thromb. Vasc. Biol.* **2003**, *23*, 2110−2115.
(26) Azizkhan, R. G.; Azizkhan, J. C.; Zetter, B. R.; Folkman, J. Mast Cell Heparin Stimulates Migration of Capillary Endothelial Cells *in vitro*. *J. Exp. Med.* **1980**, *152*, 931−944.
(27) Yang, Z. L.; Tu, Q. F.; Wang, J.; Huang, N. The Role of Heparin Binding Surfaces in the Direction of Endothelial and Smooth Muscle Cell Fate and Re-Endothelialization. *Biomaterials* **2012**, *33*, 6615−6625.
(28) Lee, H.; Dellatore, S. M.; Miller, W. M.; Messersmith, P. B. Mussel-Inspired Surface Chemistry for Multifunctional Coatings. *Science* **2007**, *318*, 426−430.
(29) Lee, B. P.; Messersmith, P. B.; Israelachvili, J. N.; Waite, J. H. Mussel-Inspired Adhesives and Coatings. *Annu. Rev. Mater. Res.* **2011**, *41*, 99−132.
(30) Lee, H.; Rho, J.; Messersmith, P. B. Facile Conjugation of Biomolecules onto Surfaces via Mussel Adhesive Protein Inspired Coatings. *Adv. Mater.* **2009**, *21*, 431−434.
(31) Bae, I. H.; Park, I. K.; Park, D. S.; Lee, H.; Jeong, M. H. Thromboresistant and Endothelialization Effects of Dopamine-Mediated Heparin Coating on a Stent Material Surface. *J. Mater. Sci: Mater. Med.* **2012**, *23*, 1259−1269.
(32) Zhu, L. P.; Yu, J. Z.; Xu, Y. Y.; Xi, Z. Y.; Zhu, B. K. Surface Modification of PVDF Porous Membranes via Poly (DOPA) Coating and Heparin Immobilization. *Colloids Surf., B* **2009**, *69*, 152−155.
(33) Liu, Y. L.; Ai, K. L.; Lu, L. H. Polydopamine and Its Derivative Materials: Synthesis and Promising Applications in Energy, Environment, and Biomedical Fields. *Chem. Rev.* **2014**, *114*, 5057−5115.
(34) Yang, Z. L.; Tu, Q. F.; Maitz, M. F.; Zhou, S.; Wang, J.; Huang, N. Direct Thrombin Inhibitor-Bivalirudin Functionalized Plasma Polymerized Allylamine Coating for Improved Biocompatibility of Vascular Devices. *Biomaterials* **2012**, *33*, 7959−7971.
(35) Li, J. A.; Li, G. C.; Zhang, K.; Liao, Y. Z.; Yang, P.; Maitz, M. F.; Huang, N. Co-Culture of Vascular Endothelial Cells and Smooth Muscle Cells by Hyaluronic Acid Micro-Pattern on Titanium Surface. *Appl. Surf. Sci.* **2013**, *273*, 24−31.
(36) Yang, Z. L.; Xiong, K. Q.; Qi, P. K.; Yang, Y.; Tu, Q. F.; Wang, J.; Huang, N. Gallic Acid Tailoring Surface Functionalities of Plasma Polymerized Allylamine-Coated 316L SS to Selectively Direct Vascular Endothelial and Smooth Muscle Cell Fate for Enhanced Endothelialization. *ACS. Appl. Mater. Inter.* **2014**, *6*, 2647−2656.
(37) Vecchia, N. F. D.; Avolio, R.; Alfè, M.; Errico, M. E.; Napolitano, A.; d'Ischia, M. Building-Block Diversity in Polydopamine Underpins a Multifunctional Eumelanin-Type Platform Tunable Through a Quinone Control Point. *Adv. Funct. Mater.* **2013**, *23*, 1331−1340.
(38) Hong, S.; Na, Y. S.; Choi, S.; Song, I. T.; Kim, W. Y.; Lee, H. Non-Covalent Self-Assembly and Covalent Polymerization Co-Contribute to Polydopamine Formation. *Adv. Funct. Mater.* **2012**, *22*, 4711−4717.
(39) Nuner, G. L.; Thomas, C. N.; Hanson, S. R.; Barry, J. J.; King, S. B.; Scott, N. A. Inhibition of Platelet-Dependent Thrombosis by Local Delivery of Heparin with a Hydrogel-Coated Balloon. *Circulation* **1995**, *92*, 1697−1700.
(40) Davie, E. W.; Fujikawa, K. Basic Mechanisms in Blood Coagulation. *Annu. Rev. Biochem.* **1975**, *44*, 799−829.
(41) Kloczewiak, M.; Timmons, S.; Lukas, T. J.; Hawiger, J. Platelet Receptor Recognition Site on Human-fibrinogen. Synthesis and Structure-Function Relationship of Peptides Corresponding to the Carboxy-Terminal Segment of the Gamma-chain. *Biochemistry.* **1984**, *23*, 1767−1774.
(42) Ding, Y. H.; Yang, Z. L.; Bi, C. W. C.; Yang, Y.; Zhang, J. C.; Xu, S. L.; Lu, X.; Huang, N.; Huang, P. B.; Leng, Y. Modulation of Protein Adsorption, Vascular Cell Selectivity and Platelet Adhesion by Mussel-Inspired Surface Functionalization. *J. Mater. Chem. B* **2014**, *2*, 3819−3829.
(43) Ding, Y. X.; Streitmatter, S.; Wright, B. E.; Hlady, V. Spatial Variation of the Charge and Sulfur Oxidation State in a Surface Gradient Affects Plasma Protein Adsorption. *Langmuir* **2010**, *26*, 12140−12146.
(44) Nie, S.; Qin, H.; Cheng, C.; Zhao, W. F.; Sun, S. D.; Su, B. H.; Zhao, C. S.; Gu, Z. Blood Activation and Compatibility on Single-molecular-layer Biointerfaces. *J. Mater. Chem. B* **2014**, *2*, 4911−4921.
(45) Li, G. C.; Yang, P.; Qin, W.; Maitz, M. F.; Zhou, S.; Huang, N. The Effect of Co-Immobilizing Heparin and Fibronectin on Titanium on Hemocompatibility and Endothelialization. *Biomaterials* **2011**, *32*, 4691−4703.
(46) Nachman, R. L.; Leung, L. L. Complex Formation of Platelet Membrane Glycoproteins IIb and IIIa with Fibrinogen. *J. Clin. Invest.* **1982**, *69*, 263−269.
(47) Agnihotri, A.; Soman, P.; Siedlecki, C. A. AFM Measurement of Interactions Between the Platelet Intergrin Receptor GPIIbIIIa and Fibrinogen. *Colloid Surf., B* **2009**, *71*, 138−147.
(48) Groth, T.; Campbell, E. J.; Herrmann, K.; Seifert, B. Application of Enzyme Immunoassays for Testing Haemocompatibility of Biomedical Polymers. *Biomaterials* **1995**, *16*, 1009−1015.
(49) Goodman, S. L.; Grasel, T. G.; Cooper, S. L.; Albrecht, R. M. Platelet Shape Change and Cytoskeletal Reorganization on Polyurethaneureas. *J. Biomed. Mater. Res.* **1989**, *23*, 105−123.
(50) McEver, R. P.; Martin, N. M. A Monoclonal Antibody to a Membrane Glycoprotein Binds Only to Activated Platelets. *J. Biol. Chem.* **1984**, *259*, 9799−9804.
(51) Nieuwenhuis, H. K.; Van Ouosterhout, J. J.; Rozemuller, E.; van Iwaarden, F.; Sixma, J. J. Studies with a Monoclonal Antibody Against Activated Platelets: Evidence that A Secreted 53,000-Molecular Weight Lysosome-Like Granule Protein is Exposed on the Surface of Activated Platelets in the Circulation. *Blood* **1987**, *70*, 838−845.
(52) Hersel, U.; Dahmen, C.; Kessler, H. RGD Modified Polymer: Biomaterials for Stimulated Cell Adhesion and Beyond. *Biomaterials* **2003**, *24*, 4382−4415.

(53) Tanaka, M.; Takayama, A.; Ito, E.; Sunami, H.; Yamamoto, S.; Shimomura, M. Effect of Pore Size of Self-Organized Honeycomb-Patterned Polymer Films on Spreading, Focal Adhesion, Proliferation, and Function of Endothelial Cells. *J. Nanosci. Nanotechnol.* **2007**, *7*, 763−772.
(54) McCormick, C.; Wadsworth, R. M.; Jones, R. L.; Kennedy, S. Prostacyclin Analogues: the Next Drug-Eluting Stent? *Biochem. Soc. Trans.* **2007**, *35*, 910−911.
(55) Sneddon, J. M.; Vane, J. R. Endothelium-Derived Relaxing Factor Reduces Platelet Adhesion to Bovine Endothelial Cells. *Proc. Natl. Acad. Sci. U.S.A.* **1988**, *85*, 2800−2804.
(56) McGrath, J. L.; Osborn, E. A.; Tardy, Y. S.; Dewey, C. F., Jr.; Hartwig, J. H. Regulation of the Actin Cycle *in vivo* by Actin Filament Severing. *Proc. Natl. Acad. Sci. U.S.A.* **2000**, *97*, 6532−6537.
(57) Gong, F. R.; Cheng, X. Y.; Wang, S. F.; Zhao, Y. C.; Gao, Y.; Cai, H. B. Heparin-Immobilized Polymers as Non-inflammatory and Non-Thrombogenic Coating Materials For Arsenic Trioxide Eluting Stents. *Acta Biomater.* **2010**, *6*, 534−546.
(58) Garas, S. M.; Huber, P.; Scott, N. A. Overview of Therapies for Prevention of Restenosis after Coronary Interventions. *Pharmacol. Ther.* **2001**, *92*, 165−178.
(59) Rajagopal, V.; Rockson, S. G. Coronary Restenosis: A Review of Mechanism and Management. *Am. J. Med.* **2003**, *115*, 547−553.
(60) Beamish, J. A.; Geyer, L. C.; Haq-Siddiqi, N. A.; Kottke-Marchant, K.; Marchant, R. E. The Effects of Heparin Releasing Hydrogels on Vascular Smooth Muscle Cell Phenotype. *Biomaterials* **2009**, *30*, 6286−6294.
(61) Gu, Z.; Rolfe, B. E.; Xu, Z. P.; Thomas, A. C.; Campbell, J. H.; Lu, G. Q. M. Enhanced Effects of Low Molecular Weight Heparin Intercalated With Layered Double Hydroxide Nanoparticles on Rat Vascular Smooth Muscle Cells. *Biomaterials* **2010**, *31*, 5455−5462.
(62) Poh, C. K.; Shi, Z. L.; Lim, T. Y.; Neoh, K. G.; Wang, W. The Effect of VEGF Functionalization of Titanium on Endothelial Cells in Vitro. *Biomaterials* **2010**, *31*, 1578−1585.
(63) Yin, M.; Yuan, Y.; Liu, C. S.; Wang, J. Development of Mussel Adhesive Polypeptide Mimics Coating for in-situ Inducing Re-Endothelialization of Intravascular Stent Devices. *Biomaterials* **2009**, *30*, 2764−2773.
(64) Yeh, E. T.; Zhang, S.; Wu, H. D.; Körbling, M.; Willerson, J. T.; Estrov, Z. Transdifferentiation of Human Peripheral Blood CD34+-Enriched Cell Population into Cardiomyocytes, Endothelial Cells, and Smooth Muscle Cells *in vivo*. *Circulation* **2003**, *108*, 2070−2073.
(65) Lavender, M. D.; Pang, Z.; Wallace, C. S.; Niklason, L. E.; Truskey, G. A. A.. A System for the Direct Co-Culture of Endothelium on Smooth Muscle Cells. *Biomaterials* **2005**, *26*, 4642−4653.
(66) Anderson, J. M.; Rodriguez, A.; Chang, D. T. Foreign Body Reaction to Biomaterials. *Semin. Immunol.* **2008**, *20*, 86−100.
(67) Jay, S. M.; Skokos, E. A.; Zeng, J.; Knox, K.; Kyriakides, T. R. Macrophage Fusion Leading to Foreign Body Giant Cell Formation Persists Under Phagocytic Stimulation by Microspheres *in vitro* and *in vivo* in Mouse Models. *J. Biomed. Mater. Res., Part A* **2010**, *93*, 189−199.
(68) Avula, M. N.; Rao, A. N.; McGill, L. D.; Grainger, D. W.; Solzbacher, F. Foreign Body Response to Subcutaneous Biomaterial Implants in a Mast Cell-Deficient $Kit^{w\text{-}Sh}$ Murine Model. *Acta. Biomater.* **2014**, *10*, 1856−1863.